Nano-probing station incorporating MEMS probes for 1D device RF on-wafer characterization

K. Daffe, J. Marzouk, A. El El Fellahi, T. Xu, Christophe Boyaval, S. Eliet, B. Grandidier, S. Arscott, Gilles Dambrine, Kamel Haddadi

HAL Id: hal-01726555
https://hal.science/hal-01726555

Submitted on 8 Mar 2018

Nano-Probing Station incorporating MEMS probes for 1D Device RF On-Wafer Characterization

K. Daffe, J. Marzouk, A. El Fellahi, T. Xu, C. Boyaval, S. Eliet,
B. Grandidier, S. Arscott, G. Dambrine and K. Haddadi

Institute of Electronics, Microelectronics and Nanotechnology (IEMN - UMR CNRS 8520) − University of Lille

Avenue Poincaré CS 60069 – 59652 Villeneuve d'Ascq Cedex – France

kamel.haddadi@univ-lille1.fr

Abstract—**A microwave nano-probing station incorporating home-made MEMS coplanar waveguide (CPW) probes was built inside a scanning electron microscope. The instrumentation proposed is able to measure accurately the guided complex reflection of 1D devices embedded in dedicated CPW micro-structures. As a demonstration, RF impedance characterization of an Indium Arsenide nanowire is exemplary shown up to 6 GHz. Next, optimization of the MEMS probe assembly is experimentally verified by establishing the measurement uncertainty up to 18 GHz.**

I. Introduction

To drive the progress of the miniaturization of electronic circuits, new metrological issues related to the dimensional and electrical characterization of nanoelectronic devices must be addressed [1]. A universal radio frequency (RF) device characterization set-up consists of a vector network analyzer (VNA), a probe station with a pair of microwave ground-signal-ground (GSG) probes aligned manually or automatically by means of a microscope or a camera system onto calibration substrates and test devices [2]. Conventional RF test structures require probing pads whose dimensions are around 50×50 µm^2 to accommodate the probe tip geometry (example: pitch of 100 µm, contact area of 30×30 µm^2). Consequently, the main barriers are: (i) the extrinsic parasitic capacitance associated with the pad that is in the order of 2 fF mask the impedance of the nanodevice, rendering de-embedding methods inaccurate [3], and (ii) the manual positioning of the probe onto the CPW test structure generates misalignment measurement errors that impact notably on the measured impedance of the nano-device itself.

Intensive research has been described in the literature to address RF metrology at the nano-scale. The first approach consists of physically accessing and using conventional on-wafer probe stations to measure nano-scale devices, using a CPW test structure that is tapered down to a few µm [4]-[5]. Although microwave potentialities of 1D and 2D nanodevices have been successfully established, this method suffers from measurement repeatability and accuracy issues for the reasons given above. The second approach gathers near-field scanning microwave microscopy (NSMM) tools that have pioneered the possibility to measure microwave impedances of one-port devices with nanometer-scale spatial resolution [6]. Basically, the NSMM consists of an atomic force microscope (AFM) combined with a microwave signal applied to the tip. The tip scans across the sample, emitting a microwave signal scattered by the material, altering its amplitude or/and phase properties. These techniques have the advantage of providing nanoscale resolution - but the distribution of the electromagnetic signals in the surrounding of the tip apex is not of TEM mode, rendering the concept of travelling waves not applicable.

The conclusions drawn from these previous studies have led us to develop a unique instrument that is a compromise between conventional on-wafer probe station and microscopy tools. We have fabricated microelectromechanical systems (MEMS) technology-based miniaturized microwave ground-signal-ground (GSG) probes [7] to achieve this. In contrast to conventional macroscopic on-wafer probing structures - micrometric CPW test structures have been designed and fabricated to accommodate the miniaturized probes and to ensure quasi-TEM mode propagation to the nano-scale devices embedded in the test structures [8]. The probes are mounted on nano-positioners and imaging is ensured by a scanning electron microscope (SEM). A detailed study on the development of the nanorobotic on-wafer probe station is given in [9] with initial RF measurements on a specially designed calibration kit up to 4 GHz.

This paper focuses on presenting results of calibrated measurements of a 1D material – an InAs nanowire using the micro-probes described in [7]-[9]. In Section II, the instrument setup is described. In Section III, the InAs nanowire deposition, and its electrical characterization (DC and RF) up to 6 GHz are established. Moreover, other results corresponding to the optimization of the measurement system are as well presented up to 18 GHz in Section IV. Finally, a brief overview of the future works relating to the design and the characterization of the new fabricated micro-probes is given.

II. Instrumental Set-up

This section provides a brief overview of the robotic on-wafer probe station developed for nano-scale device characterization. More detailed information on the system development can be found in [7]-[9]. The robotic probe station is composed of a sample stage and a micro-probing unit. The sample stage is built up with piezo-driven linear actuators manufactured by Smaract GmbH. The stage provides scanning

range of 49 mm and 103 µm respectively in X/Y and Z directions. The sample stage is also equipped with rotation capabilities. The actuators enable closed-loop operation with less than 10 nm precision in any direction. The probing unit consists of DC and microwave probers. The micro-probers are mounted also on Smaract positioners with scanning range of 16 mm in the lateral direction and 12 mm in the Z direction. Micromachined GSG micro-probes that allow contacts on 2×2 µm^2 pads are mounted on the micro-probing stages. The compact platform setup is mounted on the stage of a Tescan Mira XMU SEM. The set-up is able to determine the calibrated (and guided) *S*-parameters of CPW micro- and nano-devices with pads contacts smaller than 5 µm^2. Fig. 1 gives a comparison of main parameters between conventional and proposed on-wafer probe stations.
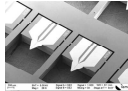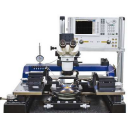

Fig. 1. Comparison between conventional and proposed on-wafer probe stations. Related probe geometries, probe positioning accuracies and probe-to-sample visualizations techniques are quantified.

The MEMS-based micro-probes are connected to the VNA coaxial cable through specially designed printed circuit board (PCB) with CPW to coaxial modes transition. Whereas the MEMS probes have shown electrical performance up to 40 GHz, the overall frequency range was limited to a few GHz because of probe assembly. Inside the SEM, a semi-rigid coaxial cable equipped with 2.92 mm coaxial connectors ensures the connection between the VNA and the probe via feedthrough. The in-house impedance standard substrate includes calibration standards that enable the reference planes of the measurements to be moved to the device-under-test (DUT). The calibration standards included on a 380 µm-thick semi-insulating Gallium Arsenide (GaAs) wafer are open, short, 50 Ω load and thru. The conductor metal used is gold (Au) of 500 nm thickness. A 20 nm-thick Nickel (Ni)-Chromium (Cr) layer was used beneath the Au to enhance adhesion to the substrate and to design the 50 Ω loads. The dimensions of the CPW were chosen to preserve a 50 Ω characteristic impedance (center conductor width = 2.3 µm, gap width = 1.8 µm and ground width = 10 µm).

III. InAs Nanowire microwave characterization

In the last decade, a growing number of researches related to the microwave measurements of devices based on carbon nanotubes (CNTs) and semiconducting nanowires (NWs) have been reported in the literature [4]-[5]. In this study, we focus on the electrical characterization of a single Indium Arsenide (InAs) nanowire embedded in a one-port CPW waveguide up to 6 GHz.

A. InAs nanowire deposition

The one-port microwave device was fabricated by incorporating the InAs NW on the CPW waveguide. The growth conditions yield NWs around 10 µm long. Consequently, the NW is directly deposited on the gap of the 50 Ω CPW waveguide (1.8 µm) without need of taper commonly found in traditional 1D device measurement methods. The device is fabricated on the in-house impedance standard substrate described in Section II considering dedicated CPW empty test structures. The NW is placed on the CPW gap using a drop of NW/isopropanol solution. The next step is to deposit an Au (500 nm) layer and pattern it with a photolithographic lift-off step to form the contacts. A SEM image of the suspended 1D device is shown in Fig. 2.
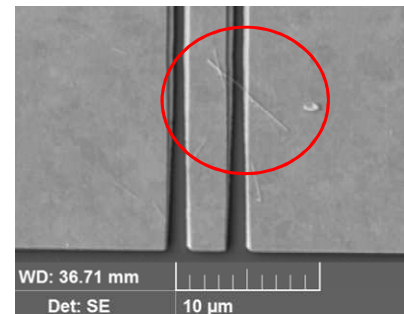

Fig. 2. SEM image of a suspended InAs nanowire embedded in a CPW test structure. The total length of the nanowire is 7.32 µm and the length of the nanowire in the suspended area is 1.11 µm.

B. InAs nanowire DC and RF characterization

The fabrication process yielded a device with an Ohmic contact at one end of the InAs NW and a Schottky-type contact at the other end. Indeed, the current-voltage (I-V) characteristic (not shown here) indicates a zero-bias rectifying Schottky diode characteristic.

The instrumental setup previously described was used for the RF characterization of the InAs NW. Using the VNA Keysight[TM] N5245A PNA-X, the RF input source power and the intermediate frequency bandwidth (IFBW) were set respectively to -10 dBm and 100 Hz. After short/open/load (SOL) vector calibration, Fig. 3 presents the extracted real and imaginary parts of the microwave impedance of the 1D device from the measured complex reflection coefficient up to 6 GHz. The measured data exhibit a resistive part in the order of few kΩ associated with a series capacitive part with reactance between -5 and -1 kΩ. It has to be noticed that the stray capacitance (between center conductor and grounds) contribute to the overall measured complex impedance. The measured reflection coefficient is then measured at various bias voltages. Fig. 4 gives a comparison between DC and dynamic (at 1 GHz) extracted conductance. From these results, we show that the dynamic conductance is around 160 times greater than its DC counterpart. The increase of the dynamic resistance is mainly attributed to the junction capacitance related to the Schottky-type contact.
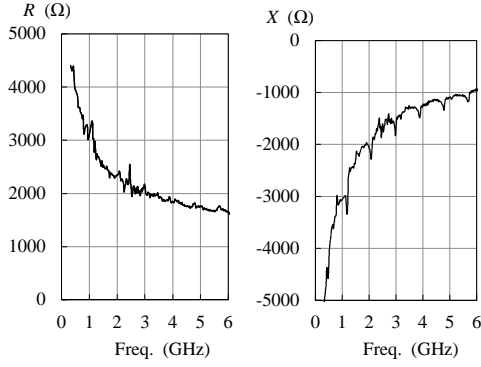
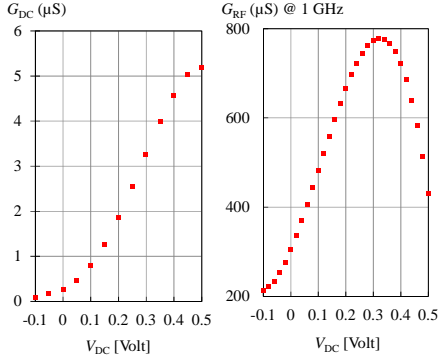Fig. 3. Measured microwave impedance $Z = R + jX$ of the InAs nanowire as a function of the frequency.

Fig. 4. Comparison between measured DC conductance G_{DC} and microwave conductance G_{RF} at 1 GHz.

IV. COMPARISON WITH ON-GOING WORK AND DISCUSSION

The frequency limit of the proposed instrumentation and results presented in Section III were related to the MEMS probe integration, in particular the optimization of the in-house PCB board that connects the coaxial cable to the MEMS probe. To expand the frequency range of operation, a new PCB board was designed and fabricated [Fig. 5(a)]. The whole probe assembly has been optimized up to 20 GHz [Fig. 5(b)].

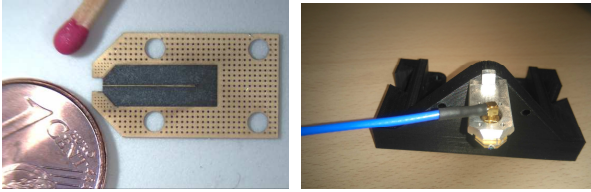(a)   (b)

Fig. 5 (a) In-house PCB for modes transition between coaxial and CPW modes. (b) Probe assembly.

Next, the measurements were conducted on the calibration standards to establish the measurement uncertainty of the set-up. The complex reflection coefficients Γ_{LOAD}, Γ_{SHORT} and Γ_{OPEN} of the calibration standards in one-port configuration are first established as follows:

-LOAD: corresponds to the measured DC resistance (by neglecting propagation effects).
-SHORT: considered ideal (full metallized structure)
-OPEN: considered ideal (probe in free-space conditions)

$$\Gamma_{LOAD} = \frac{R_{DC} - 50}{R_{DC} + 50} \quad \Gamma_{SHORT} = -1 \quad \Gamma_{OPEN} = 1 \qquad (1)$$

The first step of the characterization procedure consisted to calibrate the system in order to move the reference planes of the measurements to the semi-rigid coaxial cables inside the SEM. To do this, a SOL calibration procedure is performed at the end of the coaxial cable port using a coaxial K connector calibration kit (Model 3652, Anritsu ®). In the second step, an on-wafer multi-SOL calibrations process was achieved to extract the residual errors terms and to calibrate the measured reflection coefficient Γ up to the probe tips. The number of measurement is set to 10 for each load. The frequency step is set to 50 MHz (400 frequency points). The residual error terms consist in residual directivity (δ), reflection tracking (τ) and source match (μ). The reflection magnitude $\Delta|\Gamma|$ and phase-shift $\Delta\arg(\Gamma)$ uncertainties can be expressed as a function of the residual error terms by

$$\Delta|\Gamma| = \delta + \tau|\Gamma| + \mu|\Gamma|^2 \qquad (2)$$

$$\Delta\arg(\Gamma) = \arcsin\left(\frac{\Delta|\Gamma|}{\Gamma}\right) . \qquad (3)$$

Considering the sub-bands spanning respectively from 0.01 to 2 GHz, 2 to 8 GHz, and from 8 to 18 GHz, the measurement uncertainties are plotted in Fig. 6.
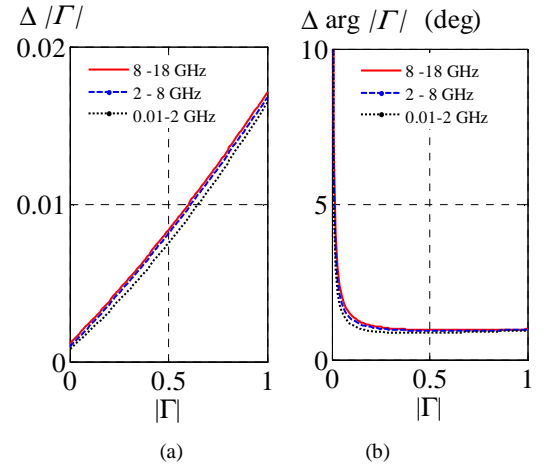

(a)   (b)

Fig. 6. Magnitude (a) and phase-shift (b) measurement uncertainties of the reflection-coefficient Γ as a function of the magnitude of Γ.

To better appreciate the measurement accuracy, the standard deviations (STD) of the complex reflection coefficient Γ is presented for the short and load standards. Although the short standard is the most reflective standard, the STD (2σ) is around $\pm$ 0.0015 up to 20 GHz as we can see in Fig. 7 (a). Concerning the load standard, Fig. 7 (b) shows a STD nearly less than 5.10^{-4} through the entire frequency band. This indicates that the micro-probes are favorable for the characterization of nano-electronic devices.
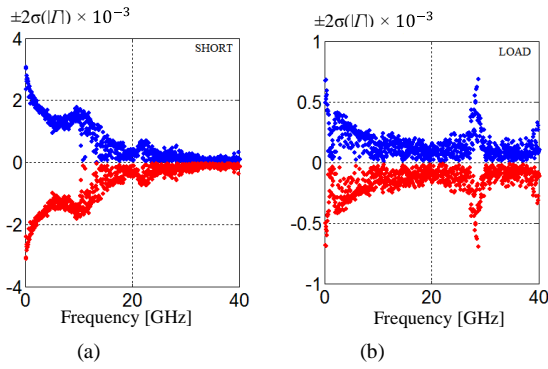
Fig. 7 Standard deviations of the reflection-coefficient Γ as a function of the frequency. The loads are "short" and "load" derived from the in-house impedance standard substrate.

Finally, to evaluate the technological variability of the in-house impedance standard substrate fabrication, we present the calibrated measurement of the reflection coefficients of two different short standards in Fig. 8.
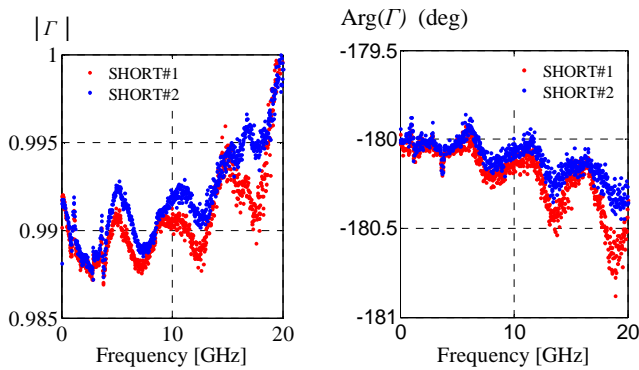

Fig. 8. Magnitude and phase-shift of the measured reflection coefficient Γ of two different short standards.

From these data, very low deviations are observed. Equivalent results have been found considering other loads.

V. PERSPECTIVE WORKS

The results altogether show that the proposed instrumentation is a viable candidate to address the need of microwave characterization technique at the nanoscale. The on-going works concern the development of two-port measurement method including two MEMS micro-probes aligned automatically by SEM vision.
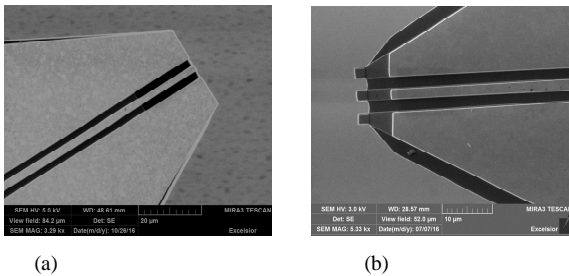

Fig. 9 SEM images showing the tips of the 1st (a) and the 2nd (b) generations of GSG micro-probes.

Other work is conducted to design and fabricated new MEMS probe generation with shrinked contact pads. Other modifications concern the use of harder meals in order to contact oxidized pads commonly found in silicon industry. First realization of these new probes generation is illustrated in Fig. 9 that gives a comparison between 1st and 2nd probes generations.

VI. CONCLUSION

Guided microwave characterization of 1D device using a dedicated nano-probing station incorporating CPW MEMS probe and built inside a scanning electron microscope has been demonstrated up to 6 GHz. Furthermore, new optimization of the proposed instrumentation extends the frequency range of operation up to 20 GHz. The instrumentation presented in this paper represents an alternative approach to conventional on-wafer methods. In particular, combination of microscopy tools, nano-positionning systems and microwave equipment is a viable alternative to tackle the issue between spatial resolution and frequency domain. In this frame, on-going works concern automation of two-port measurements, fabrication of probes with smaller dimensions and optimized contacts to address new materials measurement and increase of the frequency range.

REFERENCES

[1] The International Technology Roadmap for Semiconductors (ITRS), 2013. http://www.itrs.net/Links/2013ITRS/2013Chapters/2013ERD.pdf.

[2] A. Rumiantsev and R. Doerner, "RF Probe Technology," *IEEE Microw. Mag.*, vol. 14, pp. 46–58, 2013.

[3] K. Daffé, G. Dambrine, F. Von Kleist-Retzow and K. Haddadi, "RF wafer probing with improved contact repeatability using nanometer positioning," *87th ARFTG Microwave Measurement Conference Dig*, pp. 1–4, San Francisco, CA, 2016.

[4] K. Kim, T. Mitch Wallis, P. Rice, C.-J. Chiang, A. Imtiaz, P.Kabos and D. Filipovic, "A framework for broadband characterization of individual nanowires," *IEEE Microw. Wirel. Comp. Lett.*, vol. 20, no. 3, pp. 178–180, March 2010.

[5] Y. Zhen, and Peter J. Burke. "Microwave transport in metallic single-walled carbon nanotubes," *Nano Letters*, vol. 5, no. 7, pp. 1403–1406, 2005.

[6] A. Imtiaz, T. M. Wallis and P. Kabos, "Near-field scanning microwave microscopy: an emerging research tool for nanoscale metrology," *IEEE Microwave Magazine*, vol. 15, no. 1, pp. 52–64, 2014.

[7] A. El Fellahi, K. Haddadi, J. Marzouk, S. Arscott, C. Boyaval, T. Lasri and G. Dambrine "Integrated MEMS RF probe for SEM station - Pad size and parasitic capacitance reduction," *IEEE Microw. Wirel. Compon. Lett.*, vol. 25, no. 10, pp. 693–695, Oct. 2015.

[8] J. Marzouk, S. Arscott, A. El Fellahi, K. Haddadi, T. Lasri, C Boyaval and G. Dambrine "MEMS probes for on-wafer RF microwave characterization of future microelectronics: design, fabrication and characterization*," J. Micromech. Microeng.*, vol. 25, no 7, June 2015.

[9]   A. El Fellahi, K. Haddadi, J. Marzouk, S. Arscott, C Boyaval, T. Lasri and G. Dambrine "Nanorobotic RF probe station for calibrated on-wafer measurements,". *45th European Microw. Conf.*, Paris, France, pp. 1–4, Sept. 2015.